A normal form-based power system out-of-step protection

Nnaemeka Sunday Ugwuanyi, Xavier Kestelyn, Olivier Thomas, Bogdan Marinescu, Bin Wang

A Normal Form-based Power System Out-of-step Protection

N.S. Ugwuanyi, X. Kestelyn, , O. Thomas, B. Marinescu, , B. Wang,

***Abstract*—This paper proposes a new system-level application for monitoring out-of-step (OOS) events in power systems. As already known, amplitude-dependent frequency shift is a nonlinear phenomenon of electromechanical oscillations under large disturbances. The frequency shift indicates the system's nearness to instability. This new tool utilizes the Normal Form method to identify the named phenomenon, leading to accelerated OOS detection. The proposed strategy is illustrated and compared to the equal-area criterion method in a single-machine-infinite-bus power system. Extensive tests on IEEE 3- and IEEE 50-machine power systems prove the efficacy and potential of the proposed method for online warnings of instability and ranking of vulnerable system modes.**

***Index Terms*—Normal form, oscillation frequency drift, out-of-step prediction, transient stability.**

I. Introduction

THE he ultimate goal of any well-designed power system is to recover quickly following large disturbances such as faults, line switching, loss of large generation, e.t.c. Certain disturbances may cause the system to fail, resulting in a loss of synchronism. Out-of-step (OOS) or asynchronous operation refers to the loss of synchronism of one or more generators. OOS protection typically focuses on detecting an asynchronous operation as soon as it occurs. As a result, preventive measures such as islanding the affected generators, load-shedding, etc., are implemented.

Detecting OOS usually entails spotting significant changes in power system parameters at the start of an asynchronous action. These parameters include line impedance, rotor angle, phase, current, voltage, bus voltage frequency, e.t.c. Depending on the quantity tracked, different methods for detecting OOS exist in the literature. The authors in [1] extended the equal-area-criterion (EAC), which was previously restricted to two-machine systems, to multi-machine systems to detect OOS. This technique based on analysis of the power-angle characteristics is valuable for oscillations between two groups of generators or between an individual generator and the rest of the system. Ref. [2] employs it for OOS detection in protection applications based on power-time analysis. To find the cluster solution that gives the position leading to controlled islanding, [3] uses graph theory combined with time-domain EAC. The method's strength lies in its use of local OOS protection to detect system-wide instability. Using Clarke's transformation and analytic geometry evaluation, [4] proposes an OOS protection method. It boasts a real-time implementation that combines time-domain analysis in Clarke's domain with the sudden-change-in-voltage (SCV) approach to enhance OOS protective feature action. Zhang *et. al*, [5] convert the bus voltage phase angles obtained from phasor measurement units into a new coordinate system in which all of the bus voltage phasor ends are stable during the out-of-step oscillation process, while only the common beginning moves. The out-of-step center position criterion and the bus grouping criterion are then proposed. This method, like the wide-area measurement (WAM) methods in [6], [7], depends on the accuracy of the measurement units and the fidelity of wide-area communications to fully use it. Other existing approaches include variation in voltage frequency-based method [8], line differential current-based method [9], instantaneous active power deviation-based method [10], adaptive method [11], decision tree method [12] and turbine generator behavior-based method [13]. The majority of those references use EAC to supplement their approaches (e.g., [1]–[3], [11]), so it appears to be the most commonly published.

Most of the previous methodologies concentrate on locating the OOS incident and separating the affected generators, which means that OOS must have occurred. As a result, most of them need the fault clearing time fed as an input to the relay. They include details in the form of a switch's—YES or NO—much like time-domain simulations. They do not give sufficient information on how close the system is to going down. Some OOS symptoms are hidden but dangerous, manifesting fully solely when the only available defense may be islanding. Furthermore, most of the methods examined are local, making them incapable of detecting system-wide instability. Any method that detects the power system's gradual descent into the OOS regime in a system-wide manner will undoubtedly improve its protection. Whether current, voltage, impedance or other parameters are monitored, they all lead to one thing: controlling the natural mode of the power system. The dynamics of a power system are related to its natural mode, in addition to the subjected disturbance.

In this paper, we propose to monitor the variations in the

This study is a part of a PhD project supported by TETFUND Nigeria from 2017 to 2020. The funder's only role was to provide the funds.

N.S. Ugwuanyi is with Univ. Lille, Arts et Metiers Institute of Technology, Centrale Lille, Junia, ULR 2697 – L2EP, F-59000 Lille, France and also with Electrical/Electronic Engineering, Alex Ekwueme Federal University P.M.B. 1010, Abakaliki 480214, Nigeria (e-mail: nnaemeka.ugwuanyi@ensam.eu).

X. Kestelyn is with Univ. Lille, Arts et Metiers Institute of Technology, Centrale Lille, Junia, ULR 2697 – L2EP, F-59000 Lille, France (e-mail: Xavier.Kestelyn@ensam.eu).

O. Thomas is with Arts et Métiers Institute of Technology – LISPEN, F-59000 Lille, France (e-mail: Olivier.Thomas@ensam.eu).

B. Marinescu is with Ecole Centrale de Nantes – LS2N, F-44000 Nantes, France (e-mail: bogdan.marinescu@ls2n.fr).

B. Wang was with Texas A&M University, College Station, 77843 USA, and is now with National Renewable Energy Laboratory, Golden, 80401 USA (e-mail: bin.wang@nrel.gov).

power system's electromechanical modal parameters (in this case, oscillation frequency) prior to the commencement of the asynchronous regime to detect and mitigate the OOS. Our attention is the electromechanical dynamics, which is the principal stability effect in many systems. There are practical reasons for this proposal. As examples, the Western Interconnection power grid experienced a massive breakup on August 10, 1996. According to measurement-based research, the 0.25-Hz oscillation, which was suggestive of an imminent breakup, resulted from a gradual decrease in oscillation frequency from 0.27 Hz to 0.25 Hz, as well as a decrease in oscillation damping ratio from 7.0% to 1.2% [14]. On June 4, 2003, there was another widespread oscillation resulting from weakened system conditions. Prony analysis determined the oscillation frequency to be 0.584 Hz and the mode shape to be an east-west interaction between the Colstrip and Kemano plants, although the dominant modes for these plants are typically near 0.78 Hz and 0.63 Hz, respectively [14]. The preceding real events indicate that the reported instabilities were accompanied by a decrease in modal frequency and damping, which can help detect the onset of an OOS. When the initial conditions of a power system change, the frequency of electromechanical oscillations (EOs) changes. In a linear case, the new frequency is constant and may be viewed as a new fundamental frequency at the new initial condition. In a nonlinear scenario, the EO's frequency does not keep constant but varies with the amplitude, a phenomenon often known as a frequency shift. In this paper, we use frequency shift for the two cases and view the former as a shift for a constant amplitude. This phenomenon has piqued the interest of researchers, notably the Pacific Northwest National Laboratory, which is currently developing tools for real-time monitoring of electromechanical modes' parameters, a technology Hauer *et. al*, [14] dubbed "Mode Meter." This paper employs the Normal Form (NF) method to detect the dominant mode's frequency shift towards the asynchronous regime. The efficient detection of oscillation frequency changes will supplement existing methods and increase the power system's reliability. The strength of the proposed method lies in its ability to detect system-wide instability speedily and easily. It is so because it is not based on any particular machine, but the prevailing system condition. Controlling the responsible generators is a second step, which can be done with any other method, e.g., participation factor analysis. While identifying the exact time for OOS and the responsible generators is crucial for islanding, the proposed method boasts the capability of indicating imminent OOS before it ever occurs. This added feature is key to preventive controls. In summary, this paper's contributions include (i) a new way to estimate and monitor the oscillation frequency without repeating the small-signal analysis (SSA), (ii) a new application of Normal Form method to power system protection, (iii) the proposed OOS detection algorithm is much fast, system-wide, and has potential for real-time implementation. Moreover, the proposed tool may be coordinated to work parallel with existing tools like WAM, EAC, e.t.c., to enhance system reliability.

The rest of the paper is structured as follows: Section II discusses the theoretical foundations of the NF method. Section III provides the reader with clear motivational examples to help them understand the concept for the proposed technique. Consequently, the new method is presented. Section IV is devoted to in-depth simulations and discussions. Finally, Section V concludes the paper and suggests future research.

II. Normal Form Theories

The Poincaré and Poincé-Dulac NF theory [15] uses a polynomial transformation to simplify nonlinear differential equations. The NF method requires, to begin with, the representation of the nonlinear system with a polynomial of appropriate degree followed by a transformation that removes or simplifies the nonlinear couplings. Ref. [16] conducted detailed studies that revealed that a polynomial of degree 3 substantially retains the power system's nonlinear behavior in some vicinity of the stable equilibrium point. The NF method is particularly useful in power systems for studying the effects of modal interactions in control designs [17], [18] and power system stability [19]–[22]. This technique has also been used in vibration mechanics to investigate the frequency shift phenomenon of a natural mode subjected to a displacement [23]. The frequency shift phenomenon occurs in power systems as well, but it is not given the attention it deserves. These critical applications sparked a slew of studies aimed at easing NF's computational burden [24]–[26]. In the following subsections, the NF theory for first and second-order systems is reviewed.

A. Normal Form of First-order System

Consider a dynamical system:

$$\dot{\mathbf{x}} = \mathbf{f}(\mathbf{x}), \tag{1}$$

where $\mathbf{x}$ is the N-dimensional state vector, $\mathbf{f}$ is a smooth vector field. The system in (1) is assumed to have a stable equilibrium point at the origin, i.e. $\mathbf{f}(\mathbf{0}) = \mathbf{0}$, (otherwise, a coordinate transformation can move it to the origin) and can be approximated by Taylor series around the equilibrium point.

Therefore, system (1) can be written as:

$$\dot{\mathbf{x}} = \bar{\mathbf{A}}\mathbf{x} + \mathbf{\Gamma}(\mathbf{x}), \tag{2}$$

where $\bar{\mathbf{A}}$ is the Jacobian of $\mathbf{f}$, $\mathbf{\Gamma}(\mathbf{x})$ represents nonlinear terms expanded in polynomial series and $\mathbf{\Gamma}(\mathbf{0}) = \mathbf{0}$.

Assuming that $\bar{\mathbf{A}}$ is diagonalizable, a linear transformation $\mathbf{x} = \mathbf{\Phi}\mathbf{y}$ decouples the linear part of (2) as

$$\dot{\mathbf{y}} = \mathbf{\Lambda}\mathbf{y} + \mathbf{f}_{nl}(\mathbf{y}), \tag{3}$$

where $\mathbf{\Lambda}$ is a diagonal matrix of the eigenvalues of $\bar{\mathbf{A}}$ and $\mathbf{f}_{nl}(\mathbf{y}) = \mathbf{\Phi^T \Gamma}(\mathbf{\Phi y})$ gathers the nonlinearities in the new coordinates. $\mathbf{\Phi}$ is the right eigenvector of $\bar{\mathbf{A}}$, normalized such that $\mathbf{\Phi}^T\mathbf{\Phi} = 1$. In power systems, $\mathbf{\Lambda}$ has complex elements.

NF theorem states that if no resonance exist among the eigenvalues of $\bar{\mathbf{A}}$, there is a nonlinear transformation

$$\mathbf{y} = \mathbf{z} + \mathbf{h}(\mathbf{z}), \tag{4}$$

which simplifies the system (3) to

$$\dot{\mathbf{z}} = \mathbf{\Lambda}\mathbf{z}. \tag{5}$$

$\mathbf{h}(\mathbf{z})$ is a higher order polynomial. In other words, in (5), the counterpart of the nonlinear terms in the system (3) is removed. In the case of resonances, all mononomial terms in $\mathbf{f}_{nl}(\mathbf{y})$ that are resonant cannot be removed. NF finds $\mathbf{h}$ to eliminate the removable nonlinear terms. The NF for the first-order system has a conceptual disadvantage in that the physical meanings of the state variables may be unclear, and using second-order systems can relieve this nuisance.

B. Normal Form of Second-order Systems

The NF derivations for second-order mechanical systems have been extensively discussed in the literature and will not be replicated in this article. For details, see [23] and references therein, however, the basic steps required to understand the method are presented here. This paper will present a novel application of previous NF findings to the study of power system oscillations, inspired by the relationships between second-order mechanical and electrical models.

1) Power System Model: The equation of motion for an N-machine classical model power system can be represented by a 2nd-order differential equation (6).

$$M_i\ddot{\delta}_i + C_i\dot{\delta}_i + P_{e_i} = P_{m_i}, \tag{6}$$

$$P_{e_i} = E_i^2\mathcal{G}_{ii} + \sum_{k=1,k\neq i}^{N} E_iE_k[\mathcal{G}_{ik}\cos\delta_{ik} + \mathcal{B}_{ik}\sin\delta_{ik}].$$

$M_i, C_i, P_{e_i}, P_{m_i}, \delta_i$ are respectively inertia constant, damping constant, electrical power, mechanical power and absolute rotor angle of generator i, and $\delta_{ik} = \delta_i - \delta_k$. $\mathcal{G}_{ik}$ and $\mathcal{B}_{ik}$ are respectively the conductance and suceptance between generator i and k while E_i is the constant emf behind the transient reactance of generator i.

2) Taylor Expansion: The 3rd-order Taylor expansion of (6) for a constant input reads:

$$\begin{aligned} M_{ij}\ddot{\delta}_j + C_{ij}\dot{\delta}_j + \sum_{j=1}^{N} K_{ij}\delta_j + \sum_{j=1}^{N}\sum_{k=1}^{N} F2^i_{jk}\delta_j\delta_k + \dots \\ \sum_{j=1}^{N}\sum_{k=1}^{N}\sum_{l=1}^{N} F3^i_{jkl}\delta_j\delta_k\delta_l = 0, \end{aligned} \tag{7}$$

where $K_{ij} = \frac{\partial P_{e_i}}{\partial\delta_j}|_{\boldsymbol{\delta}=\boldsymbol{\delta_0}}$, $F2^i_{jk} = \frac{1}{2}\frac{\partial^2 P_{e_i}}{\partial\delta_j\partial\delta_k}|_{\boldsymbol{\delta}=\boldsymbol{\delta_0}}$, $F3^i_{jkl} = \frac{1}{6}\frac{\partial^3 P_{e_i}}{\partial\delta_j\partial\delta_k\partial\delta_l}|_{\boldsymbol{\delta}=\boldsymbol{\delta_0}}$. The eigenvalues of $\mathbf{K}$ are all real. In the conventional NF, the Taylor expansion of (6) has to be re-written in first-order, an operation that doubles the size of the system and leads to the computation of complex quantities.

3) Linear Transformation: Let $\mathbf{\Omega}$ be a vector of the eigenvalues, obtained by solving $(\mathbf{K} - \Omega_i^2\mathbf{M})\mathbf{\Phi}_i = \mathbf{0}$. Let the i-th element be Ω_i^2. If uniform damping is assumed, matrices $\mathbf{M}$, $\mathbf{C}$ and $\mathbf{K}$ can be diagonalized simultaneously, leading to:

$$\begin{cases} \mathbf{\Phi}_i^T\boldsymbol{M}\mathbf{\Phi}_j = \sigma_{ij} \ \ \forall i,j \\ \mathbf{\Phi}_i^T\mathbf{K}\mathbf{\Phi}_j = \Omega_i^2\sigma_{ij} \ \ \forall i,j \\ \mathbf{\Phi}_i^T\boldsymbol{C}\mathbf{\Phi}_j = 2\zeta_i\Omega_i\sigma_{ij} \ \ \forall i,j, \end{cases} \tag{8}$$

where ζ is the damping factor, and $\sigma_{ij} = 1 \ \forall i = j, \ 0 \ \forall i \neq j$. If Φ_{ip} denotes the i^{th} element of $\mathbf{\Phi}_p$ and using one generator as a reference, a linear transformation

$$\boldsymbol{\delta} = \mathbf{\Phi}\boldsymbol{y} \implies \delta_i = \Phi_{ip}y_p \tag{9}$$

transforms (7), $\forall p = 1,\dots N$, to

$$\ddot{y}_p = -\Omega_p^2 y_p - \sum_{q=1}^{N}\sum_{r=1}^{N} G^p_{qr}y_qy_r - \sum_{q=1}^{N}\sum_{r=1}^{N}\sum_{s=1}^{N} H^p_{qrs}y_qy_ry_s, \tag{10}$$

where $G^p_{qr} = F2^i_{jk}\Phi_{ip}\Phi_{jq}\Phi_{kr}, H^p_{qrs} = F3^i_{jkl}\Phi_{ip}\Phi_{jq}\Phi_{kr}\Phi_{ls}$. y is the modal variable. The damping term has been canceled in (10) by subtracting the equation corresponding to the reference generator from all other equations.

To avoid complex quantities, (10) is put to first-order using the velocity $\bar{y}_p = \dot{y}_p$ as auxiliary variable and then, each oscillator represented by a block diagonal matrix $\begin{pmatrix} 0 & 1 \\ -\Omega_p^2 & 0 \end{pmatrix}$. The auxiliary variable allows (10) to be written in the form of (3) and can always be canceled to recover 2nd-order-like oscillator equations. The first difference compared to the traditional NF method is that the 2nd-order system model is expanded by the Taylor series before putting it to first-order. The frequency of the undamped linear mode is unchanged while admitting simpler computation.

4) Nonlinear Transformation: To decouple (10), the nonlinear change of variables defined in (11) is used.

$$\begin{aligned} y_p = R_p + \sum_{i=1}^{N}\sum_{j\geq i}^{N}(a^p_{ij}R_iR_j + b^p_{ij}S_iS_j) + \sum_{i=1}^{N}\sum_{j\geq i}^{N}\sum_{k\geq j}^{N} r^p_{ijk}R_iR_jR_k \\ + \sum_{i=1}^{N}\sum_{j\geq i}^{N}\sum_{k\geq j}^{N} u^p_{ijk}R_iS_jS_k. \end{aligned} \tag{11a}$$

$$\begin{aligned} \bar{y}_p = S_p + \sum_{i=1}^{N}\sum_{j=1}^{N}\gamma^p_{ij}R_iS_j + \sum_{i=1}^{N}\sum_{j\geq i}^{N}\sum_{k\geq j}^{N}\mu^p_{ijk}S_iS_jS_k \\ + \sum_{i=1}^{N}\sum_{j\geq i}^{N}\sum_{k\geq j}^{N} v^p_{ijk}S_iR_jR_k. \end{aligned} \tag{11b}$$

R_p and S_p are new variables, respectively corresponding to the angle and speed. The unknown coefficients a^p_{ij}, b^p_{ij}, γ^p_{ij}, $u^p_{ijk}, r^p_{ijk}, v^p_{ijk}, \mu^p_{ijk}$ (equivalence of h-coefficients in first-order case), are determined by just solving sets of linear equations formulated by equating like terms. Details of their computations can be found in [23], [27, Appendix C]. Unlike the h-coefficients in (4), these coefficients are all real.

By substituting (11) into (10), followed by simplifications, the NF for the p-th mode is given by [23]:

$$\ddot{R}_p = -\Omega_p^2R_p - (A^p_{ppp} + H^p_{ppp})R_p^3 - B^p_{ppp}R_p\dot{R}_p^2, \tag{12}$$

where the coefficients A^p_{ijk} and B^p_{ijk} are the third-order residual terms expressed as $A^p_{ijk} = \sum_{l\geq i}^{N} G^p_{il}a^l_{jk} + \sum_{l\leq i}^{N} G^p_{il}a^l_{jk}$, $B^p_{ijk} = \sum_{l\geq i}^{N} G^p_{il}b^l_{jk} + \sum_{l\leq i}^{N} G^p_{il}b^l_{jk}$. Equation (12) assumes that there is no strong modal resonance, thereby neglecting the effects of cross-coupling nonlinearities. A reverse transformation is possible via (11) and (9).

III. Proposed method for out-of-step Tracking

The proposed method for OOS protection is described in this section. To begin, the reader is given clear motivational examples to help them understand the key concept that follows.

A. Motivations for the Proposed Technique

Firstly, consider a single-machine-infinite-bus (SMIB) power system whose data and model are described in Section IV-A and equation (6) respectively. It can easily be shown that if (6) is written in first-order and C is zero, its eigenvalues are given by:

$$\lambda_{1,2} = \frac{\frac{\omega_s^2}{M\omega_0^2}P_{eo} \pm j\sqrt{\left[\frac{\omega_s^2}{M\omega_0^2}P_{eo}\right]^2 - 4\frac{\omega_s^2}{M\omega_0}\frac{EV}{X_s}\cos\delta_0}}{2}, \quad (13)$$

where P_{eo} is the electrical power output of the generator, δ_0, the initial rotor angle, ω_s, the synchronous speed, and ω_0, the initial rotor speed. Note that the simplifying assumption $\omega_s = \omega_0$ was not used in (13). Equation (13) shows the effects of the generator loading on the oscillation's damping and frequency.

As reported in [28], if the generator's output increases, the frequency and damping decrease, as shown in Fig. 1a. To show this quantitatively, let the equilibrium point of the SMIB system be $15°$. The frequency of the mode is 7.82 rad/s (1.24 Hz). Using the EAC, the stability bound for this operating point is $165°$ (2.88 rad). Now, consider an initial condition ($\delta = 164.90°$, $\omega = 0$), i.e., 99.94% of the stability bound. The nonlinear response of this condition is shown in Fig. 1b. The oscillation frequency estimated from the two

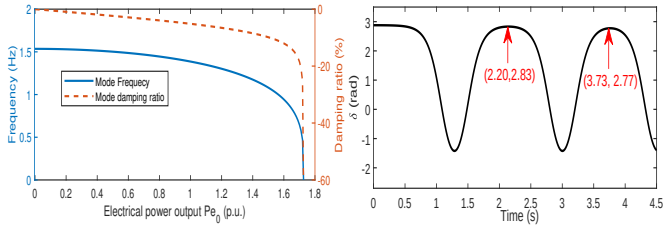

(a) (b)

Fig. 1. Power output and fault affect the frequency and damping

peaks indicated in the figure is 0.65 Hz (4.0841 rad/s), which is 48% less than the linear frequency. It implies that the two principal causes of OOS (loading and faults) manifest in decreasing the oscillation frequency.

One can, therefore, conclude that in a stable mode, the frequency decreases as the generator output or fault level increases. This frequency's descent reaches a critical point below which the mode loses stability, and the probably affected generators are those participating significantly in that oscillation mode. This phenomenon motivates the mode's stability monitoring for OOS protection.

B. Out-of-step Detection Criterion

The OOS detection criterion in this paper is quite simple and based on careful exploitation of (12). As seen in Fig. 1b, a nonlinear phenomenon of EOs under large disturbances is amplitude-dependent frequency drift. With the first-order representation, an analytical expression of the frequency shift (or *nonlinear frequency*) can be found for (12) using the perturbation methods, e.g. the multiple-scale method, as:

$$\Omega_{p_{nl}} = \Omega_p\left(1 + \frac{3(A^p_{ppp} + H^p_{ppp}) + \Omega_p^2 B^p_{ppp}}{8\Omega_p^2}\mathfrak{a}^2\right), \quad (14)$$

where $\Omega_{p_{nl}}$ is a frequency, which depends on the amplitude $\mathfrak{a}$ considered, while Ω_p is the fundamental frequency. The term in parenthesis is a correction to the fundamental frequency as the amplitude changes. Equation (14), also known as the backbone curve in mechanics, has already been derived and used to investigate the hardening and softening behavior of nonlinear structural vibration [23]. To the best of the authors' knowledge, the application of such a concept to the study of multi-machine power system oscillation is original.

Estimating the critical frequency shift necessitates an evaluation of the critical amplitude of the oscillation. Since the rotor angle δ is transformed to NF, the maximum displacement of $R = R_{cr}$ can be obtained from (12) by setting $\ddot{R} = \dot{R} = 0$ as:

$$R_{p_{cr}} = R_p = \sqrt{\frac{-\Omega_p^2}{(A^p_{ppp} + H^p_{ppp})}}, \quad (15)$$

where $R_{p_{\rm cr}}$ stands for the critical displacement of p-th NF variable, R. Since $\mathfrak{a}$ is the amplitude of the p-th mode, the critical displacement R_{pcr} has to be projected to the modal coordinate using the modal model (11a) as follows:

$$\mathfrak{a}_{p_{cr}} = y_p(R_{p_{\rm cr}}) = R_{p_{\rm cr}} + a^p_{pp}R^2_{p_{\rm cr}} + r^p_{ppp}R^3_{p_{\rm cr}}. \quad (16)$$

Therefore, the *critical frequency shift* is computed using (14) with $\mathfrak{a} = \mathfrak{a}_{p_{cr}}$. With the critical frequency shift computed, the stability is evaluated anytime as follows:

1) Obtain the system condition δ_{sc}, where sc means *system condition*.
2) Obtain the modal amplitude of the system condition using (9) as $\mathfrak{a}_{p_{sc}} = y_{p_{sc}}$.
3) With the amplitude determined, compute the frequency shift, $\Omega_{p_{nl_{sc}}}$ using (14).
4) If $\Omega_{p_{nl_{sc}}} > \Omega_{p_{nl_{cr}}}$, the system condition is considered stable; otherwise, it is unstable.

The following benefits of the proposed method are noteworthy:

- Since it is based on the oscillation mode, a system-wide parameter, it detects system-wide instability.
- It does not need the fault clearing time fed as an input to the relay, so it has a similar advantage advertised in [1].
- It requires only computations related to the mode of interest, making it fast and easy, thanks to the selective computation technique promoted in [25].
- It does not require computing the initial conditions in the NF space, so this challenging step is avoided.
- It is unnecessary to transform each system initial condition to NF space as in [19], [20].
- The impact of generator loading, load loss/addition, faults, e.t.c, on the oscillation frequency may be investigated for warnings of impending OOS.

The proposed method may incur errors due to modal interactions besides the inherent truncation error caused by Taylor expansion. Simplification to NF (12) assumes negligible effects of inter-modal interactions. This assumption is more valid for the SMIB, which has one mode or if the initial conditions for $k \neq p$ are zero for the multi-machine system. When a multi-machine power system experiences a large disturbance, the initial condition for $k \neq p$ is not zero in general, and the effect of modal interaction increases. Close

to the stability boundary, cross-coupling interactions, as well as 4^{th} and higher-order interactions, may be significant. As a result, $\Omega_{p_{nl}}$ could be slightly farther/closer, leading to a lightly conservative or optimistic outcome. A normalizing factor is added to steer the cumulative effects of all modes to the particular mode of interest, which improves the challenge of inter-modal interactions. The normalizing factor is discussed in the next paragraph.

Following the definitions in [29] for mechanical systems, the modal mass $m_p^* = \Phi_p^T \mathbf{M} \Phi_p$ is equal to the sum of (mass) $\times$ squared (mode displacement) for each mode (i.e., $m_p^* = \sum_{q=1}^{N} m_q \Phi_{pq}^2$). Similarly, the modal stiffness $k_p^* = \Phi_p^T \mathbf{K} \Phi_p$ is the sum of the strain energy stored in each oscillator, and the total strain energy indicates that $k_p^* = m_p \Omega_p^2$. Thus, we define $Tse_p = m_p \Omega_p^2$, $Tse_{p_{\text{nl}}} = m_p \Omega_{p_{\text{nl}}}^2$, where Tse_p and $Tse_{p_{\text{nl}}}$ are the total modal strain energies of the p^{th} mode at linear and nonlinear frequencies, respectively. The normalizing factor is thus defined for p-th mode as

$$S.F = \frac{Tse_{p_{\text{nl}}}}{Tse_p}. \tag{17}$$

So, for any system condition, the frequency shift is tuned as:

$$\tilde{\mathbf{\Omega}}_{nl_{\text{sc}}} = \mathbf{\Omega}_{nl_{\text{sc}}} \times S.F. \tag{18}$$

The results will later show that the proposed approach incurs tolerable errors for the considered model. In the following sections, numerical simulations are presented to test the method.

IV. Power System Case Studies

In this section, the proposed method is first illustrated with an SMIB power system and then applied on the IEEE 3- and the IEEE 50-machine power systems.

A. Case Study 1 — SMIB Power System

Consider the previously mentioned SMIB power system, which is shown in Fig. 2.

The proposed method is applied following the steps below:

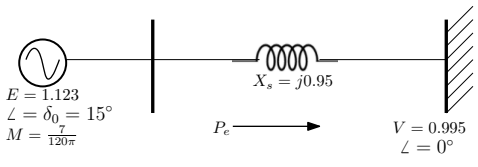

Fig. 2. Single-line diagram of a SMIB Power System

- The electrical output power $P_e = \frac{EV}{X_s} \sin \delta$.
- Evaluate the Taylor expansion terms in (7) as: $K = \frac{EV}{X_s} \cos \delta_0 = 1.1361$, $F2 = -\frac{EV}{2X_s} \sin \delta_0 = -0.1522$, $F3 = -\frac{EV}{6X_s} \cos \delta_0 = -0.1894$.
- Solve $(K - \Omega^2 M)\Phi = 0$ to get $\Omega = 7.8222$ and $\Phi = 1$.
- Use (8) and (9) to obtain the modal model (10) as: $\ddot{y} + 61.1866y - 8.1974y^2 - 10.1978y^3 = 0$.
- Following [23], compute the NF coefficients in (11) as: $a = 0.0447, b = 0.0015, \gamma = -0.0893, r = u = \mu = v = 0$, and in (12) as $A = -0.7322, B = -0.0239$.
- Therefore, the NF model (12) becomes: $\ddot{R} = -61.1866R + (0.7322 + 10.1978)R^3 - 0.0239R\dot{R}^2$.
- With $\ddot{R} = \dot{R} = 0$, evaluate the critical amplitude in R from (15) as $R_{cr} = 2.366$, and substitute into (16) to get the critical modal amplitude as: $\mathfrak{a}_{cr} = 2.366 + 0.0447 \times (2.366)^2 + 0 = 2.616$.
- With the critical modal amplitude $\mathfrak{a}_{cr}$ determined, use (14) to calculate the critical frequency shift as: $\Omega_{nl_{cr}} = 7.8222 \times \left(1 - \frac{3 \times 10.93 - 61.1866 \times 0.0239}{8 \times 61.1866} \times 2.616^2\right) = 4.0764$ rad/s.
- Therefore, the oscillation frequency should not go below 4.0764 rad/s to maintain synchronism.
- Since the SMIB has one mode only, the normalizing factor $S.F = 1$. Thus, $\tilde{\Omega}_{nl_{sc}} = \Omega_{nl_{sc}}$ for any disturbance.

Observe that the critical frequency shift we just calculated is nearly identical to the one estimated in [Fig. 1b, Section III-A].

Because it only has one mode, it may not be obvious what the NF did in the preceding example, but the job of the NF is to decouple the multi-oscillator system into separate oscillators of the type exemplified, which will be shown in next subsection.

The SMIB was subjected to various disturbances by varying the rotor angle initial condition to put the criterion to the test. The frequency shift is computed for each initial condition, and the nonlinear solution is evaluated by integrating the nonlinear model in MATLAB®. In this and subsequent sections, the nonlinear solution obtained with MATLAB® is regarded as the "true" solution. The outcomes for the various conditions are presented in Table I. For comparison, the result of the equal-area criterion is also shown. We assume the reader is familiar with the EAC method, so we leave out the specifics.

TABLE I
Comparing proposed method with EAC on SMIB power system

Post-fault (rad)	$\Omega_{nl_{cr}} = 4.0764$ rad/s $\tilde{\Omega}_{nl_{sc}}$ (rad/s)	Proposed Decision	EAC Decision	True Decision
1.7453	6.6175	Stable	Stable	Stable
2.4435	5.2168	Stable	Stable	Stable
2.6180	4.7833	Stable	Stable	Stable
2.8798	4.0705	Unstable	Stable	Stable
2.8815	–	Unstable	Unstable	Unstable

The Table shows that when the rotor angle amplitude reaches 2.8798 rad, the proposed method classifies the system as unstable because the $\tilde{\Omega}_{nl_{sc}} = 4.0705$ rad/s, which is less than the $\Omega_{nl_{cr}} = 4.0764$ rad/s. The EAC and the true solution are stable up to 2.8815 rad, implying that the proposed method is conservative with an error of only 0.06% in angle in this case. The response of the reconstructed NF, linear, and true solutions is shown in Fig. 3, confirming that the proposed method becomes unstable almost at the same time as the true solution. The NF's accuracy originates from the frequency shift against the constant frequency during a disturbance, as the linear solution assumes. It is noteworthy that if the swinging of a generator against the rest is of interest, as is the concept of multi-machine EAC [1], the proposed method will work very similarly to the EAC. Such limitations, however, are unnecessary. In the sections that follow, the proposed method will be deployed for multi-machine applications.

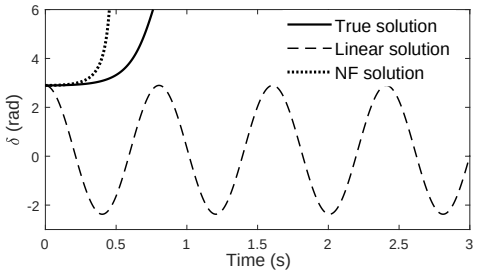

Fig. 3. Response of the system during unstable fault

B. Case Study 2 — The IEEE 3-Machine System

The IEEE 3-machine power system [30] shown in Fig. 4 has two electromechanical modes of frequencies 13.72 rad/s (Mode 1) and 8.82 rad/s (Mode 2). According to participation factor analysis, Mode 1 is most associated with generator G3, whereas Mode 2 is associated with G2. Mode 2 also has inter-area effects because it is excited regardless of the fault location. A three-phase fault was added to Bus 4, and it

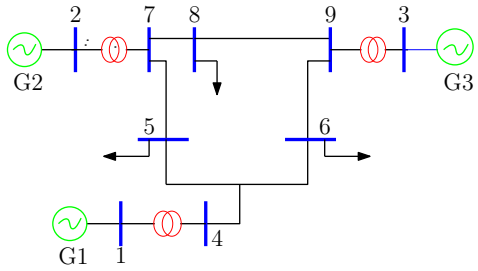

Fig. 4. One line representation IEEE 3-machine power system

was cleared over time by removing the fault until instability occurred. Mode 2 is dominant in this case. The values of $\tilde{\Omega}_{nl_{sc}}$ after each clearing time are listed in Table II. According

TABLE II
CASE STUDY 2: FAULT AT BUS 4
MODE 1 ($\Omega_{1_{nl_{\rm cr}}} = 8.55$), MODE 2 ($\Omega_{2_{nl_{\rm cr}}} = 5.44$)

Fault duration (s)	$\tilde{\Omega}_{1_{nl_{\rm sc}}}$ (rad/s)	$\tilde{\Omega}_{2_{nl_{\rm sc}}}$ (rad/s)	Proposed Decision	True Decision
0.15	13.65	8.32	Stable	Stable
0.22	13.41	6.67	Stable	Stable
0.24	13.30	5.89	Stable	Unstable
0.25	13.22	5.36	Unstable	Unstable

to Table II, the proposed method detects instability at 0.25s, while the true instability occurs at 0.24s. In this case, the results also show that for the chosen fault conditions, Mode 2 is less stable than Mode 1. This can be seen in the table, where the frequency of Mode 2 decreases faster as the stress increases, whereas the frequency of Mode 1 decreases slowly.

A second case is considered by adding a three-phase fault to Bus 9 and clearing the fault at increasing time intervals until instability occurs. Mode 1 is dominant in this case. Table III lists the values of $\tilde{\Omega}_{nl_{sc}}$ after each clearing time. According to the table, the proposed method detected instability at 0.26s, which is earlier than the true solution (i.e., 0.29s). The table also shows that Mode 1 is driving the instability in this case. The numbers in the 3rd column, i.e., $\tilde{\Omega}_{2_{nl_{sc}}}$, are the same, which appears quite ideal based on the participation factors. Notice that by observing a significant decrease in

TABLE III
CASE STUDY 2: FAULT AT BUS 9
MODE 1 ($\Omega_{1_{nl_{\rm cr}}} = 8.55$), MODE 2 ($\Omega_{2_{nl_{\rm cr}}} = 5.44$)

Fault duration (s)	$\tilde{\Omega}_{1_{nl_{\rm sc}}}$ (rad/s)	$\tilde{\Omega}_{2_{nl_{\rm sc}}}$ (rad/s)	Proposed Decision	True Decision
0.15	13.00	8.81	Stable	Stable
0.22	10.67	8.81	Stable	Stable
0.25	9.00	8.81	Stable	Stable
0.26	8.30	8.81	Unstable	Stable
0.29	–	8.81	Unstable	Unstable

the oscillation frequency, one can already tell if there is an intended OOS. The affected generators can be controlled to reinforce the system, preventing the OOS and potential blackout. Such insight is in contrast to traditional tools' YES or NO feedback.

C. Case Study 3 — IEEE 50-Machine Power System

The proposed method is tested using the IEEE 50-machine power system to show the application to large systems. A section of the test system is shown in Fig. 5. The power

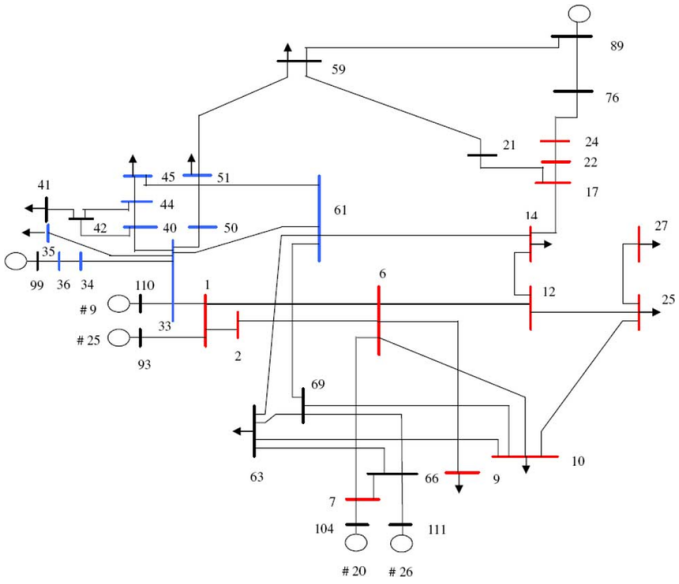

Fig. 5. Portion of one-line diagram of the IEEE 50-machine system [31]

flow data was extracted from [32], [33] while the dynamic data was taken from [34]. We know from previous studies that a fault at Bus 7 causes very high amplitude oscillation, which is primarily associated with local modes and leads to early instability. Besides, a fault at Bus 34 activates both local and inter-area modes, resulting in the simultaneous instability of several generators. Thus, two scenarios are thoroughly examined: 1) a fault on Bus 7 and 2) a fault on Bus 34.

The results of mode stability monitoring for fault at Bus 7 using the proposed method are shown in Table IV. Because mode 8 is the first to exhibit instability, only its stability is displayed in Table IV. It is discovered that Mode 8 becomes

TABLE IV
CASE STUDY 3: FAULT AT BUS 7; MODE 8 ($\Omega_{8_{nl_{\rm cr}}} = 9.05$)

Fault duration (s)	$\tilde{\Omega}_{8_{nl_{\rm sc}}}$ (rad/s)	Proposed Decision	True Decision
0.15	15.27	Unstable	Stable
0.22	11.78	Unstable	Stable
0.25	9.27	Unstable	Stable
0.26	8.33	Unstable	Stable
0.27	–	Unstable	Unstable

unstable at a time 0.26s with $\tilde{\Omega}_{8_{nl_{\rm sc}}}$ less than its critical value 9.05 rad/s. The true instability occurs at 0.27s when generator 7 (G7) loses synchronism with the rest of the system (see Fig. 6a). Mode 8 is local, and is associated most with G7 as confirmed by its shape (see Fig. 6b).

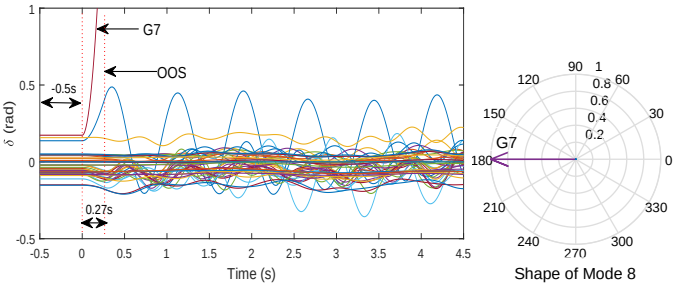

Fig. 6. (a) Trajectory at 0.27s for fault at Bus 7, (b) Shape of Mode 8

In the second case of fault at Bus 34, we observed Mode 18 and Mode 28 becoming unstable almost simultaneously, resulting in widespread instability. Table V shows the results for monitoring these two modes. The results show that synchronism is lost at 0.44s with our method because $\tilde{\Omega}_{18_{nl_{\rm sc}}}$ falls below its critical value of 8.21 rad/s (see column 2). At the same time, $\tilde{\Omega}_{28_{nl_{\rm sc}}}$ is about 1% away from its critical value, as shown in column 3. As shown in Fig. 7a, the true instant of instability is 0.40s. Mode 18 is associated with a single generator, whereas Mode 28 involves multiple generators. The shape of Mode 28, shown in Fig. 7b, confirms the separation of G1, G3, and G4 from the rest, as observed in Fig. 7a.

TABLE V
CASE STUDY 3: FAULT AT BUS 34
MODE 18 ($\Omega_{18_{nl_{\rm cr}}} = 8.21$), MODE 28 ($\Omega_{28_{nl_{\rm cr}}} = 5.76$)

Fault duration (s)	$\tilde{\Omega}_{18_{nl_{\rm sc}}}$ (rad/s)	$\tilde{\Omega}_{28_{nl_{\rm sc}}}$ (rad/s)	Proposed Decision	True Decision
0.15	13.26	9.16	Stable	Stable
0.25	12.83	8.75	Stable	Stable
0.35	11.44	7.67	Stable	Stable
0.40	9.25	6.41	Stable	Unstable
0.44	8.13	5.83	Unstable	Unstable

Table VI provides a detailed comparison of the proposed method's decisions with the true decisions for different cases. Our observation after other tests is that the method tends to be more accurate when several modes are not simultaneously excited. The maximum error in the 5$^{\rm th}$ column is 10%. However, the cases are not exhaustive, and higher errors may exist because NF results are only reliable within the approximation's validity boundary. Modern power systems also include additional equipment such as FACTS, HVDC, IBR, etc. As a result, the proposed method should be tested on such a system in the future. We emphasize that the method's strength is in the warning for impending OOS. As a result, even when the precise time eludes the proposed method, it remains faithful in indicating impending OOS. Thus, the proposed method should be used for mode instability warning signals.

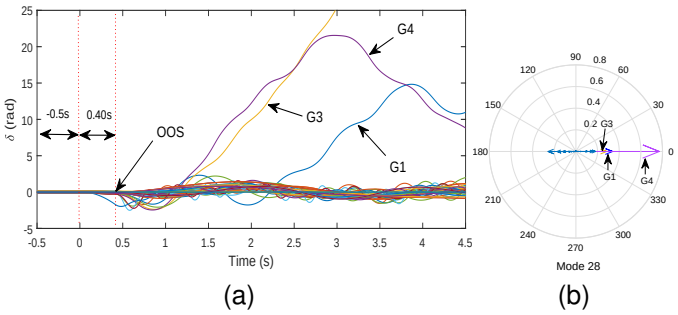

Fig. 7. (a) Trajectory at 0.40s for fault at Bus 34, (b) Shape of Mode 28

TABLE VI
ERROR ESTIMATION FOR THE PROPOSED METHOD

Fault Bus	Case	True OOS Time (s)	Proposed OOS Time (s)	Error (%)
4	Case Study 2	0.24 s	0.25 s	-4%
9	Case Study 2	0.29 s	0.26 s	+10%
7	Case Study 2	0.32 s	0.32 s	0%
5	Case Study 2	0.43 s	0.40 s	+7%
7	Case Study 3	0.27 s	0.26 s	+3%
34	Case Study 3	0.40 s	0.44 s	-10%

D. Computational Complexity and Scalability

The NF method is generally considered difficult because: (i) it needs nonlinear iterations to find the initial condition in the NF space for any considered operating point, which can be time-consuming; and (ii) it requires Taylor and modal expansions to construct its model, which is also time-consuming when considering large systems. Fortunately, the proposed method avoids these primary challenges. It does not require the computation of the initial conditions in the NF space. The NF model is constructed once and may merely be repeated if the power flow is updated. The solution to attempting a very large system (already used in [35] for systems with over 300 generators) is to reduce the network and concentrate on a specific region of the network when constructing the model. Remarkably, only the computations related to the modes of interest are necessary with our method. The computation can drastically reduce if the dominant modes are identified, and then the analysis can focus on them.

Once the NF model is constructed, the proposed tool is very speedy. It takes about 3.5 milli seconds (4$^{\rm th}$ column, Table VII) to check all the modes in the IEEE 50-machine power system with an Intel(R) Core (TM)i7-7700HQ, 2.8GHz personal computer. Construction of the NF model is the only step that takes a little longer. The total time to develop the NF model in the case of the IEEE 50-machine power system is

approximately 5.13 minutes (2.21 minutes for (6)–(7) and 2.92 minutes for (11)–(16)). As earlier noted, the NF is built once and may be updated if the power flow updates. This runtime for developing NF is not prohibitively expensive and can be performed regularly in power system operation. The proposed method is therefore useful for online applications. For very large systems, the NF model can be built offline and then used online. It should be noted that the runtime for developing NF can reduce drastically if (i) more powerful computing resources are utilized, e.g., HPC, or (ii) only selected modes are analyzed, which deserve further detailed investigations.

A computational comparison with similar works [19], [20], where the modal model (i.e, (6)–(7)) is built in first order is shown in Table VII. Indeed, avoiding first-order representation saves enormous time, especially for large systems.

TABLE VII
COMPUTATIONAL COMPARISON WITH SIMILAR WORKS

Case	[19], [20] MMT*	Proposed MMT*	Proposed OOS Assessment
Case Study 2	0.120s	0.029s	0.0017s
Case Study 3	15, 355s	132.43s	0.0035s

*MMT = time to build modal model

Fig. 8 is a pictorial representation of the necessary steps of the proposed method. The left half of the figure represents the construction of the NF model, which is a one-time process, while the right portion represents OOS monitoring and admits online operation. Because the NF method is local and based on an asymptotic expansion in the neighborhood of an equilibrium point, the NF model can be reinitialized if the power flow changes to reset the critical frequency shift. This action, however, updates all prior computations and may be an issue for online applications in terms of computation. Instead of the traditional power flow, static state estimation can be utilized to improve measurement errors. The first block in the right section, which regularly scans the system condition (i.e., checks the rotor angles), may be realized by real-time measurement tools. We have assumed that the rotor angles will be estimated correctly.

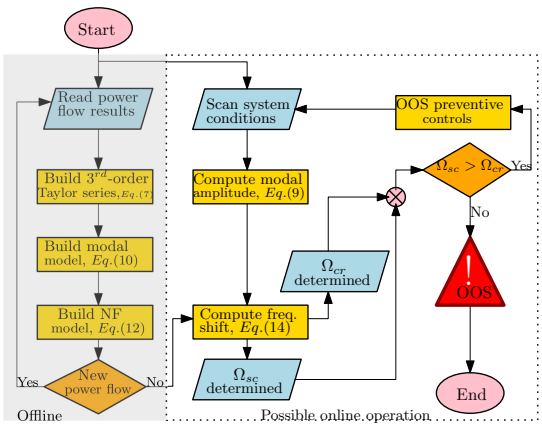

Fig. 8. Summary of the proposed method

E. Practical Significance

The proposed method has the potential for online implementation, and power system operators can use it to estimate the proximity of modes to instability quickly and roughly. The proposed approach, like many others, inherits the shortcomings of classical modeling. However, the nature of the EO is the same regardless of the model used, and detailed modeling does not significantly change the frequency of the oscillation. The inability to detect the exact time of OOS, unlike many previous schemes, does not rule the proposed tool out because the new tool can provide useful insights for controls by e.g., ranking vulnerable modes and suggesting generators to regulate based on their participation in those modes. The proposed method may also be utilized as an extra tool by power system planners to plan system operation and expansion, taking OOS mitigation measures into account. Given the current state of this study, we advocate the proposed approach as a backup tool. For practical application, the new tool can be run routinely (say every 10 minutes) in the power system operation for warning signals. Once it raises a warning flag, one can use other more robust approaches to analyze the concerned generators in detail for appropriate control actions.

F. Compatibility with Existing Tools

As stated at the outset of this article, the proposed tool may be used in conjunction with existing ones to improve system reliability. The algorithm for the majority of previous methods is as follows: Is there an OOS? If yes, isolate the responsible generators. If no, no control actions are needed. The new scheme adds more decision questions: If there is no OOS, will it occur soon? If so, control the potential generators (e.g., load-shedding). The new tool may supplement WAM techniques, in which the proposed method determines the critical frequency shift while WAM estimates the modal frequency in real-time. Since our scheme requires only the rotor angle as an input, one may use it parallel with EAC-based methods. One step of the EAC-based approach reported in [1], for example, is a fast estimation of the rotor angle, based on local measurements of voltages and currents at the generator terminal. Both methods can use the same input estimated by [1]. However, the coordination between the proposed method and the existing OOS detection scheme may be a concern that merits further investigation.

V. CONCLUSIONS

This paper expanded the real-valued Normal Form proposed in [23] to investigate practical power system oscillations. Employing second-order modeling of the power system, the NF allows multi-machine power systems decoupled as separate oscillators. A novel method for monitoring out-of-step occurrence is proposed using the NF that results. The new approach was demonstrated with an SMIB power system, which showed favorable competition compared to the well-known equal area criterion, and then applied successfully to the IEEE 3- and IEEE 50-machine power systems with promising results.

Compared to time-domain simulation, the proposed tool has a maximum error of $\pm 10\%$ and computes quickly for

tested cases. Thus, it has potential for online applications, and power system operators can use it to make a quick and rough estimation of OOS proximity and rank vulnerable modes. Therefore, the tool may provide important information leading to efficient corrective/preventive control actions. The paper considered only short-circuit scenarios, but the idea is general, as illustrated in Section III-A, and can extend to investigate other contingencies such as loss of load or generation.

Future work will compare the method with other OOS protection approaches. Strategies for pre-selecting modes to check for any disturbance should be investigated; to further reduce the computation time. The frequency shift phenomenon is general, and we envisage the extension of the proposed method to detailed models. However, with detailed generator models, putting the entire system model into the 2nd-order form can be challenging and should be re-visited.

ACKNOWLEDGMENT

This work was authored in part by the National Renewable Energy Laboratory, operated by Alliance for Sustainable Energy, LLC, for the U.S. DOE under Contract No. DE-AC36-08GO28308. The views expressed in the article do not necessarily represent the views of the DOE or the U.S. Government. The U.S. Government retains and the publisher, by accepting the article for publication, acknowledges that the U.S. Government retains a nonexclusive, paid-up, irrevocable, worldwide license to publish or reproduce the published form of this work, or allow others to do so, for U.S. Government purposes.

REFERENCES

[1] B. Alinezhad and H. K. Karegar, "Out-of-step protection based on equal area criterion," *IEEE Transactions on Power Systems*, vol. 32, no. 2, pp. 968–977, 2017.

[2] S. Paudyal, G. Ramakrishna, and M. S. Sachdev, "Application of equal area criterion conditions in the time domain for out-of-step protection," *IEEE Transactions on Power Delivery*, vol. 25, no. 2, pp. 600–609, 2010.

[3] N. Ayer and R. Gokaraju, "Online application of local oos protection and graph theory for controlled islanding," *IEEE Transactions on Smart Grid*, vol. 11, no. 3, pp. 1822–1832, 2020.

[4] J. R. Camarillo-Peñaranda, D. Celeita, M. Gutierrez, M. Toro, and G. Ramos, "An approach for out-of-step protection based on swing center voltage estimation and analytic geometry parameters," *IEEE Transactions on Industry Applications*, vol. 56, no. 3, pp. 2402–2408, 2020.

[5] S. Zhang and Y. Zhang, "A novel out-of-step splitting protection based on the wide area information," *IEEE Transactions on Smart Grid*, vol. 8, no. 1, pp. 41–51, 2017.

[6] T. Guo and J. V. Milanović, "Online identification of power system dynamic signature using pmu measurements and data mining," *IEEE Transactions on Power Systems*, vol. 31, no. 3, pp. 1760–1768, 2016.

[7] A. Sauhats, A. Utans, and E. Biela-Dailidovicha, "Wide-area measurements-based out-of-step protection system," in *2015 56th International Scientific Conference on Power and Electrical Engineering of Riga Technical University (RTUCON)*, 2015, pp. 1–5.

[8] S. Zhang and Y. Zhang, "Characteristic analysis and calculation of frequencies of voltages in out-of-step oscillation power system and a frequency-based out-of-step protection," *IEEE Transactions on Power Systems*, vol. 34, no. 1, pp. 205–214, 2019.

[9] S. M. Hashemi and M. Sanaye-Pasand, "Current-based out-of-step detection method to enhance line differential protection," *IEEE Transactions on Power Delivery*, vol. 34, no. 2, pp. 448–456, 2019.

[10] M. Rajabinasab and H. Yaghobi, "A real-time out-of-step protection strategy based on instantaneous active power deviation," *IEEE Transactions on Power Delivery*, pp. 1–1, 2020.

[11] M. A. M. Ariff and B. C. Pal, "Adaptive protection and control in the power system for wide-area blackout prevention," *IEEE Transactions on Power Delivery*, vol. 31, no. 4, pp. 1815–1825, 2016.

[12] T. Amraee and S. Ranjbar, "Transient instability prediction using decision tree technique," *IEEE Transactions on Power Systems*, vol. 28, no. 3, pp. 3028–3037, 2013.

[13] M. Abedini, M. Davarpanah, M. Sanaye-Pasand, S. M. Hashemi, and R. Iravani, "Generator out-of-step prediction based on faster-than-real-time analysis: Concepts and applications," *IEEE Transactions on Power Systems*, vol. 33, no. 4, pp. 4563–4573, 2018.

[14] J. F. Hauer, D. J. Trudnowski, and J. G. DeSteese, "A perspective on wams analysis tools for tracking of oscillatory dynamics," in *2007 IEEE Power Engineering Society General Meeting*, 2007, pp. 1–10.

[15] H. Poincaré, *Les mthodes nouvelles de la mcanique cleste*. Paris: Gauthiers- Villars, 1892. [Online]. Available: http://henripoincarepapers.univ-lorraine.fr/chp/hp-pdf/hp1892mna.pdf

[16] B. Wang, X. Xu, and K. Sun, "Power system transient stability analysis using high-order taylor expansion systems," in *2019 IEEE Texas Power and Energy Conference, TPEC 2019*. College Station, TX, USA: IEEE, 2019.

[17] H. Lomei, M. Assili, D. Sutanto, and K. Muttaqi, "A New Approach to Reduce the Non-Linear Characteristics of a Stressed Power System by Using the Normal Form Technique in the Control Design of the Excitation System," *IEEE Transactions on Industry Applications*, vol. 53, no. 1, pp. 492 – 500, 2017.

[18] S. Liu, A. R. Messina, and V. Vittal, "Assessing placement of controllers and nonlinear behavior using normal form analysis," *IEEE Transactions on Power Systems*, vol. 20, no. 3, pp. 1486–1495, 2005.

[19] B. Wang and K. Sun, "Nonlinear Modal Decoupling of Multi-Oscillator Systems With Applications to Power Systems," *IEEE Access*, vol. 6, pp. 9201–9217, 2018.

[20] B. Wang, K. Sun, and X. Xu, "Nonlinear modal decoupling based power system transient stability analysis," *IEEE Transactions on Power Systems*, vol. 34, no. 6, pp. 4889–4899, 2019.

[21] T. Tian, X. Kestelyn, O. Thomas, H. Amano, and A. R. Messina, "An Accurate Third-Order Normal Form Approximation for Power System Nonlinear Analysis," *IEEE Transactions on Power Systems*, vol. 33, no. 2, pp. 2128–2139, 2018.

[22] H. Amano, T. Kumano, T. Inoue, and H. Taniguchi, "Proposal of nonlinear stability indices of power swing oscillation in a multimachine power system," *Electrical Engineering in Japan*, vol. 151, no. 4, pp. 16–24, 2005.

[23] C. Touzé, O. Thomas, and A. Chaigne, "Hardening/softening behaviour in non-linear oscillations of structural systems using non-linear normal modes," *Journal of Sound and Vibration*, vol. 273, no. 1-2, pp. 77–101, 2004.

[24] N. S. Ugwuanyi, X. Kestelyn, and B. Marinescu, "Power System Nonlinear Modal Analysis Using Computationally Reduced Normal Form Method," *Energies*, vol. 13, no. 5, p. 1249, 2020.

[25] N. S. Ugwuanyi, X. Kestelyn, O. Thomas, B. Marinescu, and A. R. Messina, "A New Fast Track to Nonlinear Modal Analysis of Power System Using Normal Form," *IEEE Trans. on Power Systems.*, vol. 35, no. 4, pp. 3247–3257, 2020.

[26] M. Hernandez and A. R. Messina, "Recursive linearization of higher-order for power system models," *IEEE Transactions on Power Systems*, pp. 1–1, 2020.

[27] C. Touzé, "A normal form approach for nonlinear normal modes. [Research Report] Publications du LMA, numéro 156, LMA. ¡hal-01154702¿," Publications du LMA, numéro 156, LMA.¡hal-01154702¿, Tech. Rep., 2003.

[28] B. Wang and K. Sun, "Formulation and Characterization of Power System Electromechanical Oscillations," *IEEE Transactions on Power Systems*, vol. 31, no. 6, pp. 5082–5093, 2016.

[29] O. Matsushita, M. Tanaka, H. Kanki, M. Kobayashi, and P. Keogh, *Modal Analysis of Multi-Degree-of-Freedom Systems*. Tokyo: Springer Japan, 2017, pp. 41–78.

[30] P. W. Sauer and M. A. Pai, *Power system dynamics and stability*. New Jersy: Prentice Hall, 1998.

[31] Y. Xu, Z. Y. Dong, R. Zhang, Y. Xue, and D. J. Hill, "A decomposition-based practical approach to transient stability-constrained unit commitment," *IEEE Transactions on Power Systems*, vol. 30, no. 3, pp. 1455–1464, 2015.

[32] R. D. Zimmerman and C. E. Murillo-Sanchez, "MATPOWER (Version 7.0) [Software]," 2019. [Online]. Available: https://matpower.org

[33] R. D. Zimmerman, C. E. Murillo-Sánchez, and R. J. Thomas, "Matpower: Steady-state operations, planning, and analysis tools for power

systems research and education," *IEEE Transactions on Power Systems*, vol. 26, no. 1, pp. 12–19, 2011.

[34] S. Liu, "Assessing placement of controllers and nonlinear behavior of electrical power system using normal form information," Ph.D. dissertation, Iowa State University Ames,, 2006.

[35] V. Vittal, W. Kliemann, D. G. Chapman, A. D. Silk, Y. Xni, and D. J. Sobajic, "Determination of generator groupings for an islanding scheme in the manitoba hydro system using the method of normal forms," *IEEE Transactions on Power Systems*, vol. 13, no. 4, pp. 1345–1351, 1998.